

Weakly Supervised Tracklet Person Re-Identification by Deep Feature-wise Mutual Learning

Zhirui Chen^{1,2}, Jianheng Li^{1,3}, Wei-Shi Zheng^{1,3*}

¹School of Data and Computer Science, Sun Yat-sen University, China

²Accuvision Technology Co.,LTD

³Key Laboratory of Machine Intelligence and Advanced Computing, Ministry of Education, China
chenzhr5@mail2.sysu.edu.cn, lijheng3@mail2.sysu.edu.cn, wszheng@ieee.org

Abstract

The scalability problem caused by the difficulty in annotating Person Re-identification(Re-ID) datasets has become a crucial bottleneck in the development of Re-ID. To address this problem, many unsupervised Re-ID methods have recently been proposed. Nevertheless, most of these models require transfer from another auxiliary fully supervised dataset, which is still expensive to obtain. In this work, we propose a Re-ID model based on Weakly Supervised Tracklets(WST) data from various camera views, which can be inexpensively acquired by combining the fragmented tracklets of the same person in the same camera view over a period of time. We formulate our weakly supervised tracklets Re-ID model by a novel method, named deep feature-wise mutual learning(DFML), which consists of Mutual Learning on Feature Extractors (MLFE) and Mutual Learning on Feature Classifiers (MLFC). We propose MLFE by leveraging two feature extractors to learn from each other to extract more robust and discriminative features. On the other hand, we propose MLFC by adapting discriminative features from various camera views to each classifier. Extensive experiments demonstrate the superiority of our proposed DFML over the state-of-the-art unsupervised models and even some supervised models on three Re-ID benchmark datasets.



Figure 1. Tracklets separate because of tracking error, which can be inexpensively combined to WST by human annotators.

1. Introduction

The objective of person re-identification(Re-ID) is to recognize people across non-overlapping surveillance camera views. Benefiting from deep learning in recent years, the performance of Re-ID models has achieved significant progress [1, 18, 19]. However, a crucial bottleneck of current person Re-ID is the limited scalability problem due to the fully supervised annotation Re-ID datasets. In the context of conventional supervised Re-ID, we need to annotate person bounding box images and label the positive or negative image pairs across different camera views. It is quite expensive for the reason that (1) we have no knowledge of where and when the person that occurred in one camera view occurs in other camera views, and (2) human annotators are hard to remember such a large number of person images.

To address the scalability problem in Re-ID, many recent works have focused on unsupervised person re-identification [7, 26, 13]. However, existing unsupervised

*Corresponding author.

learning Re-ID methods are not quite competitive compared with the supervised Re-ID methods, because it is difficult to learn robust and discriminative features in the absence of pairwise label guidance.

In this paper, we consider a weakly supervised person Re-ID learning problem, that leverages the weakly supervised person tracklets data from a surveillance video. As is shown in Fig. 1, it is inevitable that raw person tracklets would be fragmented even if they belong to the same person because of occlusion, motion blur, scale variation, and other tracking errors. Thus, we refer to the weakly supervised tracklets (WST) by combining the raw person tracklets, which belong to the same person during annotation. This annotation is quite inexpensive, because in most cases we only combine the raw person tracklets within a very short time on the same camera view.

Furthermore, we leverage WST to our deep feature-wise mutual learning. First, we propose a “two feature extractors” architecture design where two networks learn from each other mutually. Second, we propose a multiple feature classifiers architecture design where learning information delivers among classifiers so that they can learn from each other.

We summarize our contributions as follows:

1. We refer to weakly supervised tracklets (WST) by combining the raw tracklets from the same person, within a narrow space-time area.
2. We formulate our deep feature-wise mutual learning (DFML) by way of Mutual Learning on Feature Extractors (MLFE) and Mutual Learning on Feature Classifiers (MLFC).
3. Our proposed DFML achieves competitive performance in three widely used benchmarks, and ablation experiments demonstrate the effectiveness of MLFE and MLFC.

2. Related Work

2.1. Person Re-ID

2.1.1 Supervised Re-ID Learning

With the development of deep learning in recent years, significant improvements have been made in the person Re-ID field, specifically, supervised person Re-ID. In the early years, because of the limitation of the size of person Re-ID datasets, researchers tended to train a pairwise siamese network [14, 25], where a binary-classification model is optimized with a pair of person images as input and a probability is output that indicated whether the two images belong to the same person. Later, with the increasing scale of datasets, many works [30, 31, 32] treated the training of per-

son Re-ID as an image classification problem, in which all images of the same person are regarded as the same class.

2.1.2 Unsupervised Re-ID Learning

Recently, supervised person Re-ID has encountered several tricky issues, such as expensive annotations of persons and domain adaptation problems. These problems led to the appearance of a special type of unsupervised person Re-ID, where a model is trained on a labeled dataset (source domain), and then knowledge is transferred to another unlabeled dataset (target domain). Some methods [7, 26] adopted clustering to assign a pseudo label to unlabeled person images in the self-training framework, while others [6, 23] used GAN to generate target images with a similar style of images from the source domain. Li et al. [13] began with the special temporal and spatial characteristic of person Re-ID, assuming that the positive tracklet pairs are not available, even on the same camera view. Our motivation is similar to theirs, but we assume that for the same person under the same camera view, a tracklet may be truncated into multiple tracklets due to tracking errors. These errors are easily corrected by a human annotator.

2.1.3 Weakly Supervised Re-ID Learning

Several works focused on the weakly supervised learning for person Re-ID. In person search, a sub field of person Re-ID, the gallery is a raw scene image, rather than the cropped bounding box. To some extent, it is a weakly supervised setting. However, methods of person search require full supervised annotation for the training of person detection. The setting proposed by Meng et al. [16] is closer to weakly supervised learning, where we only access the multiple video-based person label, namely the persons occurred in the video, but their respective tracklets. In a similar way, Wang et al. [21] proposed a large weakly supervised Re-ID dataset where they replaced image-level annotations with bag-level annotations.

2.2. Deep Mutual Learning

Hinton et al. first introduced knowledge distillation [9], transferring the knowledge from teacher networks (big networks) to student networks (small networks), to improve the performance of the student network. However, Zhang et al. found that it doesn't require a small network as the student network. It also worked well on a student network with the same scale as the teacher network. Therefore they proposed deep mutual learning, where two networks learn from each other at the same time [28]. The method proposed in this work is similar to deep mutual learning. The main difference is that, deep mutual learning proposed by Zhang et al. is “predict-wise” learning while ours is “feature-wise”

learning, which will be explained in details in the following section.

3. Proposed Method

3.1. Problem Setting and Overview

Let $\{x_i, y_i, c_i\}_{i=1}^N$ denotes the training set, where x_i is a person bounding box image in WST labeled y_i collected in camera view labeled c_i ; $y_i = 1, \dots, M_{c_i}$, where M_{c_i} is the number of WST from camera view c_i ; $c_i = 1, \dots, C$, where C is the number of camera views. In our weakly supervised tracklet formulation, raw person tracklets extracted from the same camera view, are combined into one WST during label annotation if they correspond to the same person. Thus, y_i indicates an independent person label under a specific camera view c_i ; therefore, we also call y_i a person label in the remainder of this paper. In contrast to fully supervised Re-ID, in our weakly setting we are unaware of the mapping relation of the same person across various camera views in the training set, which is a crucial challenge in our problem setting.

Our goal is to learn a deep discriminative feature representation model for Re-ID matching, which is the essential objective of Re-ID. In the following, to introduce our Deep Feature-wise Mutual Learning (DFML), we first introduce a baseline method.

3.2. Our Baseline Model

Li et al. proposed Per-Camera Tracklet Discrimination (PCTD) learning [13]. Specifically, the model of PCTD formulates C distinct classification tasks within C camera views in a multi-branch network architecture design. These C classification tasks share a ResNet-50 network backbone [8] as a feature extractor but have their individual fully connected layer as a classifier branch.

Inspired by PCTD, we propose our baseline model for Weakly Supervised Tracklet Person Re-Identification, which is more appropriate and more effective for our problem formulation.

3.2.1 Per-Camera Learning

In our baseline model, we formulate C distinct classification tasks, which share a ResNet-50 network backbone and have their individual classifier branches. As is shown in Fig. 2, we adopt two FC layers as a classifier branch, with a BN layer [10] followed by the first FC layer in each classifier branch. Then, the softmax Cross-Entropy (CE) loss function is used to optimize each classification task. The CE loss of the i -th sample is computed as follows:

$$L_{ce}(x_i) = -\log P_{y_i}(x_i) \quad (1)$$

where $P_{y_i}(x_i) \in \mathbb{R}$ is the y_i -th element of $P(x_i)$, and $P(x_i) \in \mathbb{R}^{M_{c_i}}$ is the output of the softmax layer in classifier branch c_i , as shown in Fig. 2.

Given a mini-batch χ , we formulate the Per-Camera Learning as follows:

$$L_{PL}^0 = \frac{1}{\|\chi\|} \sum_{x_i \in \chi} L_{ce}(x_i) \quad (2)$$

3.2.2 Cross-Camera Learning

In the context of Re-ID, a person should only be discriminated by his visual appearance irrespective of the circumstances that he is in and the cameras that he is caught. Thus, the discriminative feature of the person image should be independent of the camera view. We assume that the distribution of people from different camera views is equivalent. It is difficult and even impossible to learn the features that meet the equivalent distribution of various camera view. Here we simply focus our attention on the restriction of features' arithmetic means. To this end, the arithmetic means of discriminative features obtained from each camera view should be pulled closer during the training phase. Thus, we formulate the Cross-Camera Learning as follows:

$$L_{CL}^0 = \sum_{u \neq v} \frac{\|\mu_u - \mu_v\|_2^2}{C_{batch} \times (C_{batch} - 1)} \quad (3)$$

$$\mu_u = \frac{1}{\|\chi_u\|} \sum_{x_i \in \chi_u} f_{x_i} \quad (4)$$

where $f_{x_i} \in \mathbb{R}^{2048}$ is the discriminative feature extracted by the feature extractor; χ_u is the images set from camera view u in a mini-batch; $\mu_u \in \mathbb{R}^{2048}$ is the mean of those features from camera view u in a mini-batch; C_{batch} is the number of camera views in a mini-batch, and $C_{batch} \times (C_{batch} - 1)$ is a normalization factor.

Based on the above analysis, we formulate our baseline model as follows:

$$L_{baseline} = L_{PL}^0 + \lambda L_{CL}^0 \quad (5)$$

where λ is the weight coefficient to balance Per-Camera Learning and Cross-Camera Learning.

3.3. Mutual Learning on Feature Extractors (MLFE)

In conventional deep mutual learning [28], there are two individual networks, and these networks do not share any weight parameters. Zhang et al. proposed a loss function to compute the Jensen-Shannon Divergence of the two networks' predicts (generated after the softmax layer), where both of predicts are obtained from the same input image. During the back-propagation in training, the two networks'

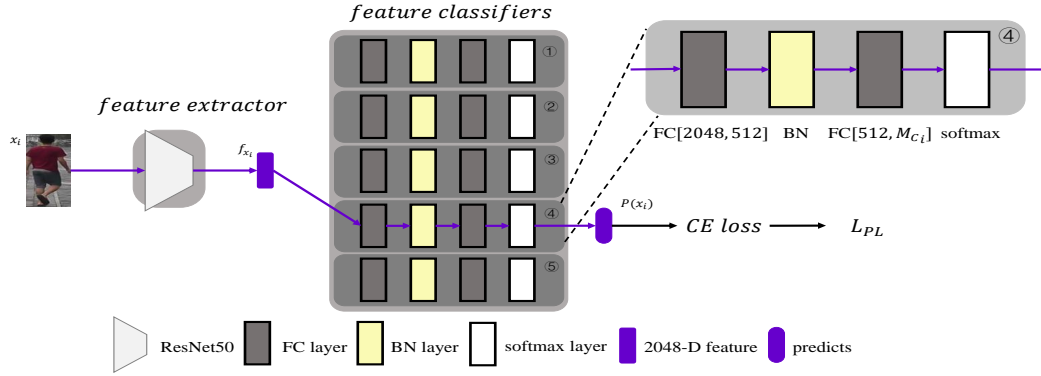


Figure 2. An overview of our Weakly Supervised Tracklet Re-ID baseline model. This is a case for 5 camera views which correspond to 5 classifier branches, respectively. A person image from the 4th camera view is fed into the feature extractor for obtaining the feature. Then, the feature is fed into the 4th branch for obtaining the predicts, which is used to compute L_{PL} .

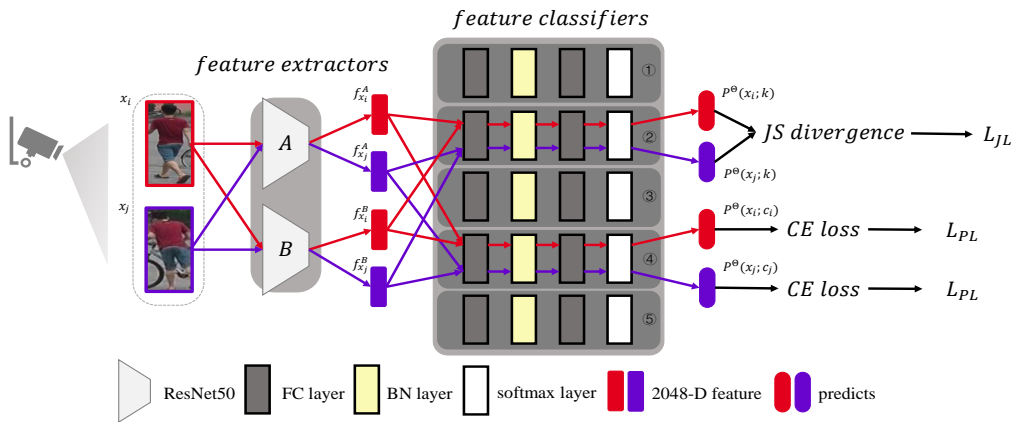


Figure 3. An overview of our DFML model. There are two images of the same person from the 4th camera view. The red stream corresponds to the forward propagation of the first image, while the purple stream corresponds to the second image. All of the extracted features are fed into the 4th branch to compute L_{PL} . Additionally, the features of the two images are fed into other branches (e.g. the 2nd branch) to compute L_{JL} .

parameters would update depending on both networks' predicts. Consequently, the two networks learn from each other mutually, which achieves the deep mutual learning design. In Zhang's experiment, this design performed better than a single network design. In this way, deep mutual learning is guided by the predicts, which we call it "predict-wise" mutual learning.

In contrast, our work achieves the deep mutual learning design in a "feature-wise" manner, which is guided by discriminative features. As shown in Fig. 3, we also adopt the two networks design. Based on our aforementioned baseline model in Per-Camera Learning, we leverage two networks to extract discriminative features, and both networks are followed by the same cluster of M_{c_i} classifier branches that correspond to the M_{c_i} classification tasks. With two networks design, the predicts $P(x_i)$ is rewritten by $P^\Theta(x_i)$, as are L_{ce}^Θ and L_{PL}^Θ . Specifically, they are formulated as follows:

$$L_{ce}^\Theta(x_i) = -\log P_{y_i}^\Theta(x_i) \quad (6)$$

$$L_{PL}^\Theta = \frac{1}{\|\mathcal{X}\|} \sum_{x_i \in \mathcal{X}} L_{ce}^\Theta(x_i) \quad (7)$$

where $\Theta \in \{A, B\}$ is a network label, and $P_{y_i}^\Theta(x_i) \in \mathbb{R}$ is the y_i -th element of $P^\Theta(x_i)$.

In summary, We formulate our Mutual Learning on Feature Extractors as follows:

$$L_{PL} = \frac{1}{2}(L_{PL}^A + L_{PL}^B) \quad (8)$$

Most conventional deep learning models for person Re-ID also consist of a feature extractor followed by a feature classifier. Specifically, in the conventional deep learning model for person Re-ID, discriminative features $f_a, f_b, f_c \dots$ extracted by the feature extractor, which correspond to the person images of the same person label, would be classified as the same label by the feature classifier. In this way, after it updates the network weight parameter during the training phase, $f_a, f_b, f_c \dots$ would be closer

in terms of Euclidean distance or cosine distance. Thus, we can re-identify a person by the Euclidean distance or cosine distance between discriminative features during the test phase.

In our MLFE, discriminative features $f_{x_i}^A$ and $f_{x_i}^B$ are both classified by the same classifier in branch c_i , and they are classified as the same label y_i . According to the above analysis, it actually makes $f_{x_i}^A$ and $f_{x_i}^B$ closer during the training phase. In other words, with feature $f_{x_i}^A$ closing to $f_{x_i}^B$ and $f_{x_i}^B$ closing to $f_{x_i}^A$, it makes the learning information deliver between network A and network B mutually, which indicates that they learn from each other mutually. Our mutual learning is guided by discriminative features; thus it is a “feature-wise” method. In the following, we introduce Mutual Learning on Feature Classifiers, where classifier branches learn from each other guided by discriminative features.

3.4. Mutual Learning on Feature Classifiers (MLFC)

Recalling Per-Camera Learning in the above section, we note that updating the parameter weights of the C classifier branches depends on the different discriminative features corresponding to the C camera views respectively during the training phase, and different classifier branches do not depend on the same discriminative feature in this design. In other words, we adapt feature f_{x_i} to classifier branch c_i , but we do not adapt f_{x_i} to other classifier branches $k(k \neq c_i)$, which implies that the discrimination ability of different classifier branches would be extremely partial to their corresponding camera view after the training phase. However, we cannot adapt feature f_{x_i} to classifier branch $k(k \neq c_i)$ directly, because the mapping relation of the person label between camera view c_i and camera view $k(k \neq c_i)$ is unknown and the person with label y_i in camera view c_i may not exist in camera view k .

To this end, we adapt feature f_{x_i} to other classifier branches in an elegant way during the training phase, which achieves our MLFC. When we leverage f_{x_i} as a discriminative feature input to classifier branch $k(k \neq c_i)$, it outputs a result of predicts of the person in camera view k . As analyzed above, we have no knowledge of which person label in camera view k is the correct predict; thus, we cannot propagate the loss during back-propagation within the training phase. Nevertheless, we can feed another feature f_{x_j} , where $c_j = c_i$ and $y_i = y_j$, into classifier branch k , and obtain another predicts. After that, we pull these two predicts closer, which achieves feature adaption across camera views.

Formally, we define a pair set as follows:

$$\rho = \{(x_i \in \chi, x_j \in \chi) \mid c_i = c_j, y_i = y_j, i \neq j\} \quad (9)$$

We extend the predicts $P^\Theta(x_i)$ to $P^\Theta(x_i; k)$, which

means the predicts of the classifier branch k . We leverage Kullback Leibler (KL) Divergence to measure the distance between two predicts of a pair of images x_i and x_j within the branch k :

$$D_{KL}^\Theta(x_i, x_j; k) = \sum_{l=1}^{M_k} P_l^\Theta(x_j; k) \times \log \frac{P_l^\Theta(x_j; k)}{P_l^\Theta(x_i; k)} \quad (10)$$

where $P_l^\Theta(x_j; k) \in \mathbb{R}$ is the l^{th} element of $P^\Theta(x_j; k)$.

KL Divergence is an asymmetrical distance metric, while a symmetrical distance metric is more appropriate. We adopt Jensen-Shannon (JS) Divergence, a symmetrical distance metric, which is based on KL Divergence.

$$D_{JS}^\Theta(x_i, x_j; k) = \frac{1}{2} D_{KL}^\Theta(x_i, x_j; k) + \frac{1}{2} D_{KL}^\Theta(x_j, x_i; k) \quad (11)$$

In a mini-batch, we compute the arithmetic mean of all $D_{JS}^\Theta(\cdot)$ in the pair set ρ , which formulates our MLFC for feature adaption across camera views. Specifically, it is formulated as follows:

$$L_{JL}^\Theta = \sum_{(x_i, x_j) \in \rho} \sum_{k=1}^C \frac{D_{JS}^\Theta(x_i, x_j; k)}{C \times \|\rho\|} \quad (12)$$

where $C \times \|\rho\|$ is a normalization factor.

When it is applied to the two networks design introduced in the last section, we can obtain the following:

$$L_{JL} = \frac{L_{JL}^A + L_{JL}^B}{2} \quad (13)$$

If MLFC is absent, different classifier branches would not be fed by the same features. With MLFC, different classifier branches would depend on the same features when updating the weight parameters in the training phase, which indicates that learning information would deliver among these classifiers. Namely, they learn from each other mutually by the guidance of these same features, which we also call “feature-wise” manner.

3.5. Model Training and Testing

To summarize, the objective function of our model is formulated as follows:

$$L = L_{PL} + \lambda L_{CL} + \gamma L_{JL} \quad (14)$$

where λ and γ control the relative importance of the three objective losses, and L_{CL} is expanded from one network to two networks:

$$L_{CL} = \frac{L_{CL}^A + L_{CL}^B}{2} \quad (15)$$

where the formulations of L_{CL}^A and L_{CL}^B are similar to that of L_{CL}^0 .

Table 1. Basic information statistics of the datasets

Dataset	#ID	#Train	#Test	#Image
MARS	1,261	625	636	1,191,003
Market-1501	1,501	751	750	32,668
DukeMTMC-ReID	1,812	702	1,110	36,411

Table 2. Statistics of # Weakly Supervised Tracklet(WST) in the training split

Dataset	#images	#Original Tracklets	#WST
MARS	509,914	8,298	1,955
Market-1501	12,936	-	3,262
DukeMTMC-ReID	16,522	-	2,196

In the testing phase, the final similarity between two image is computed as follows:

$$s(x_i, x_j) = \frac{\cos_sim(f_{x_i}^A, f_{x_j}^A) + \cos_sim(f_{x_i}^B, f_{x_j}^B)}{2} \quad (16)$$

4. Experiments

4.1. Experimental Setting

4.1.1 Datasets

We evaluate our model on a widely used video-based person Re-ID benchmark dataset MARS [30], and on two image-based person Re-ID datasets, Market-1501 [31] and DukeMTMC-ReID [17]. In our experiment, we adopt the standard train/test splits of these datasets shown in Table 1.

4.1.2 Training and Evaluation Protocol

We assume all person images per ID per camera were drawn from a single pedestrian track, as this assumption is usually used in recent studies [13, 12]. This assumption may not always be true in academic datasets, and we have a discussion in section 4.5.1.

In the training split of MARS, there are 8,298 original tracklets. To obtain WSTs, we combine the tracklets that have the same original person label and the same camera view label in MARS. In the training splits of Market-1501 and DukeMTMC-ReID, there are 12,936 and 16,522 images, respectively, but no original tracklet. We also combine the images that have the same original person label and the same camera view label into one WST. Table 2 shows the statistics of the number of WSTs. During the training phase, we do not use any original person labels in these three datasets.

In the test splits of MARS, Market-1501 and DukeMTMC-ReID, we adopt the standard single query evaluation protocol in these three datasets, and there are no differences from the common supervised person Re-ID.

Table 3. Comparison on Market-1501

Supervision	Method	Rank-1(%)	mAP(%)
Unsupervised	CycleGAN	48.1	20.7
	PUL	50.9	24.8
	CAMEL	54.5	26.3
	TJ-AIDL	58.2	26.5
	HHL	62.2	31.4
	TAUDL	63.7	41.2
	MAR	67.7	40.0
	UTAL	69.2	46.2
	ECN	75.1	43.0
Weakly Supervised	DFML(ours)	81.29	56.47
Supervised	MSCAN	80.31	57.53
	DF	81.0	63.4
	SSM	82.21	68.80
	SVDNet	82.3	62.1
	GAN	83.97	66.07
	PCB	92.4	77.3

Mean average precision (mAP) and Rank-1 will be adopted to measure the performance.

4.2. Implementation Details

We implemented our model in the PyTorch framework. We adopt ResNet-50 [8] pretrained on ImageNet [5] as network A and network B . All person images are resized to 256×128 using bilinear interpolation. We set the batch size as $B=64$ and select these 64 images in a special random way as described below. To ensure that we have an adequate number of images in a single camera view and make μ_u more accurate in Eq. (4), we only select images from two camera views in a mini-batch, with 32 images per camera view. To make ρ in Eq. (9) have more elements, we randomly select 16 pairs of images from per camera view mentioned above separately, for which each pair of images has the same person label. We set weight coefficient $\lambda = 0.2$ and $\gamma = 0.4$. For model optimization, we adopt the ADAM algorithm with an incipient learning rate of 5×10^{-4} with the two moment terms $\beta_1 = 0.9$ and $\beta_2 = 0.999$.

4.3. Comparisons with the State-of-the-Art Methods

We evaluate our model against different kinds of methods, including unsupervised methods(CycleGAN [37], PUL [7], CAMEL [26], TJ-AIDL [22], HHL [35], TAUDL [12], MAR [27], DAL [4], UTAL [20], ECN [36]), weakly supervised methods(UTAL [20]) and supervised methods(MSCAN [11], DF [29], OIM [24], QAN [15], SSM [2], SVDNet [18], Snippet [3], PAN [34], GAN [33], PCB [19]).

We compare our model with 10 state-of-the-art unsupervised methods on three datasets. From results shown in Table 3, 4, 5, our model achieves higher accuracy on both image-based datasets and video-based datasets than those unsupervised methods. On Market-1501 dataset, the

Table 4. Comparison on DukeMTMC-ReID

Supervision	Method	Rank-1(%)	mAP(%)
Unsupervised	PUL	36.5	21.5
	CycleGAN	38.5	19.9
	TJ-AIDL	44.3	23.0
	HHL	46.9	27.2
	TAUDL	61.7	43.5
	UTAL	62.3	44.6
	ECN	63.3	40.4
	MAR	67.1	48.0
Weakly Supervised	DFML(ours)	68.17	47.12
Supervised	GAN	67.68	47.13
	OIM	68.1	-
	PAN	71.6	51.5
	SVDNet	76.7	56.8
	PCB	81.9	65.3

Table 5. Comparison on MARS

Supervision	Method	Rank-1(%)	mAP(%)
Unsupervised	TAUDL	43.8	29.1
	DAL	46.8	21.4
	UTAL	49.9	35.2
Weakly Supervised	UTAL(weakly)	59.5	51.7
	DFML(ours)	63.91	52.02
Supervised	QAN	73.7	51.7
	Snippet	86.3	76.1

Table 6. Ablation study of MLFE and MLFC on Market-1501

method	MLFE	MLFC	Rank-1(%)	mAP(%)
Our Baseline(without L_{cl})	✗	✗	66.33	40.78
Our Baseline	✗	✗	72.06	44.69
DFML	✗	✓	78.74	52.68
	✓	✗	72.35	45.76
	✓	✓	81.29	56.47

best unsupervised method, ECN, is lower than ours by up to 6% in Rank-1, and the number reaches 14% for UTAL on MARS dataset. Moreover, most of these unsupervised methods require other annotation data for auxiliary learning, while our weakly supervised annotation only needs little cost.

Compared with supervised learning methods, our method seems still competitive. For example, NSCAN and DF are inferior to ours on Market-1501 dataset, while GAN and OIM are inferior to our method on DukeMTMC-ReID dataset.

Because of the variety of weakly supervised settings, we only compare our method with the latest proposed UTAL whose setting is close to ours. Table 5 shows that our method is superior to UTAL by 4.4% in Rank-1 on MARS dataset. The result validates the effectiveness of our method again.

4.4. Ablation Study

We conduct an ablation experiment to demonstrate the effectiveness of both MLFE and MLFC.

As shown in Table 6, when MLFE is absent, the performance decreases by 2.55%(81.29%-78.74%) in Rank-1 on Market-1501. The main reason for this result is that without two networks restricting and learning from each other, the feature learned by one network would adapt to their corresponding camera view space in haste. Therefore the general view information will be weaker, which certainly decreases the performance.

On the other hand, when MLFC is absent, the performance decreases by 8.94%(81.29%-72.35%). The main reason is that without feature adaption across different camera views, the Re-ID spaces of different camera views do not fuse very well.

4.5. Further Analysis

4.5.1 Reduced Dataset

In most circumstances of the real-world, a persons pass by a camera view only once withing a very long time(or never return), and it is approximately true on DukeMTMC-ReID but there are some exceptions in Market-1501 and MARS. Market-1501 and MARS are originated from the same source videos, thus here we only have a discussion on Market-1501.

To make Market-1501 more realistic, we reduce Market-1501 in the following way: if the time difference of two person images that belong to the same camera view and the same person is within x minutes(e.g. 3 minutes or 5 minutes), we assume they belong to the same WST. Then we have one or more WSTs per person per camera view. We reserve the longest WST per person per camera view, and remove the other WST. In this way, we have two datasets named Market-1501-3min-WST and Market-1501-5min-WST respectively, which is shown in Table 8.

Our experiment on these two datasets, which is shown in Table 9, indicated that we still got a considerable performance of Rank-1 74.91% and Rank-1 77.08%. Note that the number of person images of these two datasets is just 77.8% and 81.64% of the original Market-1501. This result validates the effectiveness of our method again.

4.5.2 More Networks on MLFE

We explore the use of more than two networks in MLFE. As shown by the experiment results in Table 7, compared with the two networks design in MLFE, the three networks design achieves the similar performance, which indicates that too many networks restricting each other in MLFE may not lead to better performance. Therefore, two networks design is sufficient in our MLFE.

Table 7. Comparison with more networks on Market-1501

method	Rank-1(%)	mAP(%)
DFML(without MLFE,one network)	78.74	52.68
DFML(two networks)	81.29	56.47
DFML(three networks)	81.08	57.86

Table 8. #images of Market1501-3min-WST and Market1501-5min-WST in the training split

DataSet	#images	remaining rate(%)
Market-1501	12,936	100
Market-1501-3min-WST	10,065	77.8
Market-1501-5min-WST	10,564	81.64

Table 9. performance of Market1501-3min-WST and Market1501-5min-WST

DataSet	Rank-1(%)	mAP(%)
Market-1501-3min-WST	74.91	49.08
Market-1501-5min-WST	77.08	52.26

4.5.3 Large Number of Camera Views

When there are too many camera views in the training dataset, MLFC would clearly be slow because we should adapt the discriminative feature to too many classifiers of other camera views. To mitigate this problem, for a person image of camera view i , we only adapt the respective feature to the classifier of the camera view k in which the person occurred in camera view i usually occurs. For example, camera A is quite close to camera B but far away from camera C in the real world. Persons occurred in camera view A would usually occur in camera view B but not camera view C ; thus, we could adapt the discriminative feature from camera A to the classifier of camera B but not camera C . Specifically, we define the following probability function:

$$\phi(i, j) = P(\text{occur in view } i | \text{occur in view } j) \quad (17)$$

Briefly, $\phi(i, j)$ is the probability that a person occurs in camera view i in the condition of this person occurring in camera view j . Then we rewrite MLFC formulated as follows:

$$L_{JLM}^{\ominus} = \sum_{(x_i, x_j) \in \rho} \sum_{k=1}^C \frac{\mathbb{1}(\phi(k, c_i) \geq \eta) D_{JS}^{\ominus}(x_i, x_j; k)}{\|\rho\| \times \sum_{k=1}^C \mathbb{1}(\phi(k, c_i) \geq \eta)} \quad (18)$$

where η is the probability threshold and $\|\rho\| \times \sum_{k=1}^C \mathbb{1}(\phi(k, c_i) \geq \eta)$ is a normalization factor. Specially, $\eta = 0$ means we adopt the original MLFC, and $\eta = 1$ means MLFC is absent.

$$L_{JLM} = \frac{L_{JLM}^A + L_{JLM}^B}{2} \quad (19)$$

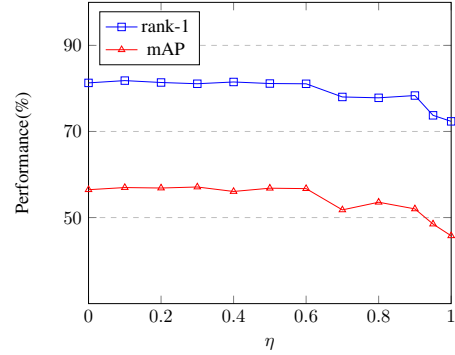


Figure 4. Performance of various η on Market-1501

In this way, we obtain the loss function L_{JLM} of the formulation where we only adapt the discriminative feature of person image to the classifier of the camera view in which this person occurs with a certain probability.

As a matter of fact, it is difficult to obtain the exact value of $\phi(\cdot)$ in the real world. We can roughly estimate it according to some indirect factor, such as the distance between cameras. To demonstrate how our MLFC works, we use the fully supervised annotation of datasets to obtain the exact value of $\phi(\cdot)$ in the following experiment.

In contrast to our full model, we replace L_{JL} with L_{JLM} in this experiment. The experiment shown in Fig. 4 reveals the performance sensitivity of threshold η on Market-1501, from which we observe that we can also obtain a high performance in our model where η is approximately less than 0.6. Thus, in real-world applications, it is unnecessary for a discriminative feature to adapt to every classifier branch, and we only adapt the discriminative feature of a person image to the classifier of the camera views in which this person occurs usually.

5. Conclusion

In this work, we proposed a novel Deep Feature-wise Mutual Learning (DFML) model for weakly supervised tracklet person re-identification. This model learns from Weakly Supervised Tracklet (WST) data, obtained from combining the fragmented video person tracklets of the same person in the same camera view over a period of time. In contrast to fully supervised Re-ID data, our WST is quite cheaper to obtain, which enables our DFML to be more scalable in real-world applications. Our proposed DFML consists of Mutual Learning on Feature Extractors (MLFE) and Mutual Learning on Feature Classifiers (MLFC), where MLFC makes feature more adaptive to each camera view and MLFE makes feature more robust and discriminative. Extensive experiments demonstrate the superiority of our proposed DFML over the state-of-the-art unsupervised models, and even some supervised Re-ID models.

References

- [1] Ejaz Ahmed, Michael Jones, and Tim K Marks. An improved deep learning architecture for person re-identification. In *Proceedings of the IEEE conference on computer vision and pattern recognition*, pages 3908–3916, 2015.
- [2] Song Bai, Xiang Bai, and Qi Tian. Scalable person re-identification on supervised smoothed manifold. In *Proceedings of the IEEE Conference on Computer Vision and Pattern Recognition*, pages 2530–2539, 2017.
- [3] Dapeng Chen, Hongsheng Li, Tong Xiao, Shuai Yi, and Xiaogang Wang. Video person re-identification with competitive snippet-similarity aggregation and co-attentive snippet embedding. In *Proceedings of the IEEE Conference on Computer Vision and Pattern Recognition*, pages 1169–1178, 2018.
- [4] Yanbei Chen, Xiatian Zhu, and Shaogang Gong. Deep association learning for unsupervised video person re-identification. *arXiv preprint arXiv:1808.07301*, 2018.
- [5] Jia Deng, Wei Dong, Richard Socher, Li-Jia Li, Kai Li, and Li Fei-Fei. Imagenet: A large-scale hierarchical image database. In *Proceedings of the IEEE Conference on Computer Vision and Pattern Recognition*, pages 248–255, 2009.
- [6] Weijian Deng, Liang Zheng, Qixiang Ye, Guoliang Kang, Yi Yang, and Jianbin Jiao. Image-image domain adaptation with preserved self-similarity and domain-dissimilarity for person re-identification. In *Proceedings of the IEEE Conference on Computer Vision and Pattern Recognition*, pages 994–1003, 2018.
- [7] Hehe Fan, Liang Zheng, Chenggang Yan, and Yi Yang. Unsupervised person re-identification: Clustering and fine-tuning. *ACM Transactions on Multimedia Computing, Communications, and Applications (TOMM)*, 14(4):83, 2018.
- [8] Kaiming He, Xiangyu Zhang, Shaoqing Ren, and Jian Sun. Deep residual learning for image recognition. In *Proceedings of the IEEE Conference on Computer Vision and Pattern Recognition*, pages 770–778, 2016.
- [9] Geoffrey Hinton, Oriol Vinyals, and Jeff Dean. Distilling the knowledge in a neural network. *arXiv preprint arXiv:1503.02531*, 2015.
- [10] Sergey Ioffe and Christian Szegedy. Batch normalization: Accelerating deep network training by reducing internal covariate shift. *arXiv preprint arXiv:1502.03167*, 2015.
- [11] Dangwei Li, Xiaotang Chen, Zhang Zhang, and Kaiqi Huang. Learning deep context-aware features over body and latent parts for person re-identification. In *Proceedings of the IEEE Conference on Computer Vision and Pattern Recognition*, pages 384–393, 2017.
- [12] Minxian Li, Xiatian Zhu, and Shaogang Gong. Unsupervised person re-identification by deep learning tracklet association. In *Proceedings of the European Conference on Computer Vision (ECCV)*, pages 737–753, 2018.
- [13] Minxian Li, Xiatian Zhu, and Shaogang Gong. Unsupervised tracklet person re-identification. *IEEE transactions on pattern analysis and machine intelligence*, 2019.
- [14] Wei Li, Rui Zhao, Tong Xiao, and Xiaogang Wang. Deepreid: Deep filter pairing neural network for person re-identification. In *Proceedings of the IEEE conference on computer vision and pattern recognition*, pages 152–159, 2014.
- [15] Yu Liu, Junjie Yan, and Wanli Ouyang. Quality aware network for set to set recognition. In *Proceedings of the IEEE Conference on Computer Vision and Pattern Recognition*, pages 5790–5799, 2017.
- [16] Jingke Meng, Sheng Wu, and Wei-Shi Zheng. Weakly supervised person re-identification. In *Proceedings of the IEEE Conference on Computer Vision and Pattern Recognition*, pages 760–769, 2019.
- [17] Ergys Ristani, Francesco Solera, Roger Zou, Rita Cucchiara, and Carlo Tomasi. Performance measures and a data set for multi-target, multi-camera tracking. In *Proceedings of the European Conference on Computer Vision (ECCV)*, pages 17–35, 2016.
- [18] Yifan Sun, Liang Zheng, Weijian Deng, and Shengjin Wang. Svdnet for pedestrian retrieval. In *Proceedings of the IEEE International Conference on Computer Vision*, pages 3800–3808, 2017.
- [19] Yifan Sun, Liang Zheng, Yi Yang, Qi Tian, and Shengjin Wang. Beyond part models: Person retrieval with refined part pooling (and a strong convolutional baseline). In *Proceedings of the European Conference on Computer Vision (ECCV)*, pages 480–496, 2018.
- [20] Jiajie Tian, Zhu Teng, Rui Li, Yan Li, Baopeng Zhang, and Jianping Fan. Imitating targets from all sides: An unsupervised transfer learning method for person re-identification. *arXiv preprint arXiv:1904.05020*, 2019.
- [21] Guangrun Wang, Guangcong Wang, Xujie Zhang, Jianhuang Lai, and Liang Lin. Weakly supervised person re-identification: Cost-effective learning with A new benchmark. *arXiv preprint arXiv:1904.03845*, 2019.
- [22] Jingya Wang, Xiatian Zhu, Shaogang Gong, and Wei Li. Transferable joint attribute-identity deep learning for unsupervised person re-identification. In *Proceedings of the IEEE Conference on Computer Vision and Pattern Recognition*, pages 2275–2284, 2018.
- [23] Longhui Wei, Shiliang Zhang, Wen Gao, and Qi Tian. Person transfer gan to bridge domain gap for person re-identification. In *Proceedings of the IEEE Conference on Computer Vision and Pattern Recognition*, pages 79–88, 2018.
- [24] Tong Xiao, Shuang Li, Bochao Wang, Liang Lin, and Xiaogang Wang. Joint detection and identification feature learning for person search. In *Proceedings of the IEEE Conference on Computer Vision and Pattern Recognition*, pages 3415–3424, 2017.
- [25] Dong Yi, Zhen Lei, Shengcai Liao, and Stan Z Li. Deep metric learning for person re-identification. In *2014 22nd International Conference on Pattern Recognition*, pages 34–39, 2014.
- [26] Hong-Xing Yu, Ancong Wu, and Wei-Shi Zheng. Cross-view asymmetric metric learning for unsupervised person re-identification. In *Proceedings of the IEEE International Conference on Computer Vision*, pages 994–1002, 2017.
- [27] Hong-Xing Yu, Wei-Shi Zheng, Ancong Wu, Xiaowei Guo, Shaogang Gong, and Jian-Huang Lai. Unsupervised per-

- son re-identification by soft multilabel learning. In *Proceedings of the IEEE Conference on Computer Vision and Pattern Recognition*, pages 2148–2157, 2019.
- [28] Ying Zhang, Tao Xiang, Timothy M Hospedales, and Huchuan Lu. Deep mutual learning. In *Proceedings of the IEEE Conference on Computer Vision and Pattern Recognition*, pages 4320–4328, 2018.
- [29] Liming Zhao, Xi Li, Yueting Zhuang, and Jingdong Wang. Deeply-learned part-aligned representations for person re-identification. In *Proceedings of the IEEE International Conference on Computer Vision*, pages 3219–3228, 2017.
- [30] Liang Zheng, Zhi Bie, Yifan Sun, Jingdong Wang, Chi Su, Shengjin Wang, and Qi Tian. Mars: A video benchmark for large-scale person re-identification. In *Proceedings of the European Conference on Computer Vision (ECCV)*, pages 868–884, 2016.
- [31] Liang Zheng, Liyue Shen, Lu Tian, Shengjin Wang, Jingdong Wang, and Qi Tian. Scalable person re-identification: A benchmark. In *Proceedings of the IEEE international conference on computer vision*, pages 1116–1124, 2015.
- [32] Liang Zheng, Hengheng Zhang, Shaoyan Sun, Manmohan Chandraker, Yi Yang, and Qi Tian. Person re-identification in the wild. In *Proceedings of the IEEE Conference on Computer Vision and Pattern Recognition*, pages 1367–1376, 2017.
- [33] Zhedong Zheng, Liang Zheng, and Yi Yang. Unlabeled samples generated by gan improve the person re-identification baseline in vitro. In *Proceedings of the IEEE International Conference on Computer Vision*, pages 3754–3762, 2017.
- [34] Zhedong Zheng, Liang Zheng, and Yi Yang. Pedestrian alignment network for large-scale person re-identification. *IEEE Transactions on Circuits and Systems for Video Technology*, 2018.
- [35] Zhun Zhong, Liang Zheng, Shaozi Li, and Yi Yang. Generalizing a person retrieval model hetero-and homogeneously. In *Proceedings of the European Conference on Computer Vision (ECCV)*, pages 172–188, 2018.
- [36] Zhun Zhong, Liang Zheng, Zhiming Luo, Shaozi Li, and Yi Yang. Invariance matters: Exemplar memory for domain adaptive person re-identification. In *Proceedings of the IEEE Conference on Computer Vision and Pattern Recognition*, pages 598–607, 2019.
- [37] Jun-Yan Zhu, Taesung Park, Phillip Isola, and Alexei A Efros. Unpaired image-to-image translation using cycle-consistent adversarial networks. In *Proceedings of the IEEE international conference on computer vision*, pages 2223–2232, 2017.